

Simplified optical configuration for a sloshing-speedmeter-enhanced gravitational wave detector

Andreas Freise,^{1,*} Haixing Miao,¹ and Daniel D. Brown²

¹*School of Physics and Astronomy and Institute for Gravitational Wave Astronomy,
University of Birmingham, Edgbaston, Birmingham B15 2TT, United Kingdom*

²*Department of Physics and The Institute of Photonics and Advanced Sensing (IPAS) University of Adelaide, SA,
5005, Australia, and OzGrav, Australian Research Council Centre of Excellence for Gravitational Wave Discovery*

(Dated: April 3, 2024)

We propose a new optical configuration for an interferometric gravitational wave detector based on the speedmeter concept using a sloshing cavity. Speedmeters provide an inherently better quantum-noise-limited sensitivity at low frequencies than the currently used Michelson interferometers. We show that a practical sloshing cavity can be added relatively simply to an existing dual-recycled Michelson interferometer such as Advanced LIGO.

Current interferometric gravitational wave detectors such as LIGO, Virgo, GEO or KAGRA [1–4] are based on modified Michelson interferometers. The design for future gravitational wave observatories such as the Einstein Telescope [5] requires the use of more advanced quantum-noise-reduction techniques.

The Michelson interferometer is sensitive to the difference in position of the end test masses. The concept of the speedmeter refers to interferometer configurations whose main output signal is proportional to the speed of the end test masses instead. Speedmeters by themselves cannot provide quantum-noise reduction at the desired level. Both position- and speedmeters can be improved by additional optical systems, such as for example squeezed light and filter cavities. However, the speedmeters provide an inherently better quantum-noise-limited sensitivity at low frequencies, and thus might lead to less complex designs for future detectors. In this paper we discuss a new variant of the speedmeter concept and investigate practical issues of this configuration. Based on the idea of using a so-called sloshing cavity to turn a Michelson interferometer into a speedmeter, we investigate alternative optical configurations for coupling the sloshing cavity to the main interferometer. In particular we show a new configuration that is equivalent to previously proposed in terms of quantum-noise reduction, but features fewer additional optics. We briefly discuss the length noise requirements for the sloshing cavity.

I. SLOSHING MICHELSON AS A SPEEDMETER

The concept of using a so-called sloshing cavity with a Michelson interferometer to generate a speedmeter was first introduced by Purdue and Chen [6]. The optical layout of one version of this scheme is shown in Figure 1. The Advanced LIGO layout is retained, using

a Signal Recycling Mirror (SRM) with different transmissivity, see below, and the output light is coupled to a so-called sloshing cavity. The coupling beam splitter (CM) allows some light to reach the output, while some light is directed back and forth between the interferometer and the sloshing cavity. Another mirror (M1) is used to close the other open port.

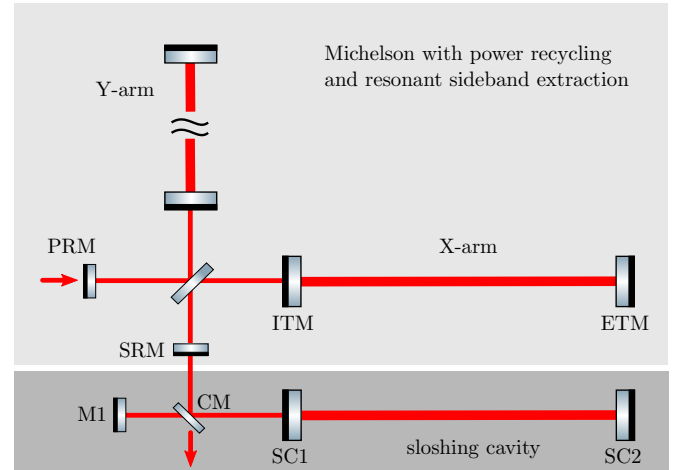


Figure 1. Optical layout of one possible Advanced LIGO design with a sloshing cavity as described in [6] (sloshing RSE MI).

With the correct tuning of transmissions and position of the new optics, the sloshing cavity returns the signal light back into the interferometer, such that the relative mirror positions are measured again at a different time, and the light leaking out from CM to the output produces a speedmeter signal, see [6] for a detailed description.

In the following we will refer to this setup as *original sloshing RSE MI* (sloshing resonant-sideband extraction Michelson). In this setup the SRM transmissivity has been set equal to that of the Input Test Masses (ITMs) of the interferometer arms, and they form an impedance matched cavity. This modifies the interferometer response such that the signal light does not experience a frequency dependent change due to the signal recycling

* andreas.freise@ligo.org

cavity or the arm cavity, i.e. $T_{\text{SRC}} = 1$. This choice provides intuitive mathematical descriptions but does not represent an optimal optical design, as we will show below. The original proposal should be understood as a conceptual design that introduces the idea rather than a practical design. For example, the longitudinal and alignment degrees of freedom of each additional mirror must be controlled by feedback systems to very high precision (as with all main optical elements of the Michelson interferometer). A simple optical layout with fewer optics will significantly help with designing feedback systems without introducing additional disturbances or unwanted coupling between optics.

parameter	aLIGO reference	orig. sloshing DRMI	sloshing alternative 1	sloshing alternative 2
power in	125 W	125 W	250 W	125 W
arm power	770 kW	770 kW	770 kW	770 kW
BS power	5.5 kW	5.5 kW	100 kW	5.5 kW
L_{arm}	3995 m	3995 m	3995 m	3995 m
T_{PRM}	0.03	0.03	0.0072	0.03
T_{ITM}	0.014	0.014	0.22	0.014
T_{ETM}	5 ppm	5 ppm	5 ppm	5 ppm
F_{arm}	450	450	24	450
T_{SRM}	0.2	0.014	1	0.2
T_{SRC}	0.22	1	1	0.22
Ω	-	$2\pi \cdot 200$ Hz	$2\pi \cdot 200$ Hz	$2\pi \cdot 200$ Hz
δ	-	$2\pi \cdot 750$ Hz	$2\pi \cdot 750$ Hz	$2\pi \cdot 750$ Hz
T_{CM}	-	0.063	0.996	0.996
T_{SC1}	-	0.0011	1	1
T_{SC2}	-	0	0	0
F_{SC}	-	5600	5600	5600

Table I. Optical parameters of the example setups discussed in this paper: a) the Advanced LIGO reference design and b) the original sloshing cavity setup as shown in Figure 1. In addition the parameters for two new alternative configurations are shown, see the main text for a detailed description.

For comparing the quantum-noise performance of the interferometer it is useful to define the bandwidth of the interferometer by the transmissivities of the coupling mirror (CM) and the sloshing cavity input mirror (SC1) (see also Appendix A):

$$\Omega = \frac{c\sqrt{T_{\text{SC1}}}}{2L} \quad (1)$$

and

$$\delta = cT_{\text{CM}}/L \quad (2)$$

with L the length of the interferometer arms, which is also the length of the sloshing cavity.

In practice we have a desired or required values for δ and Ω from which we can compute the transmissivities of the sloshing cavity optics as:

$$T_{\text{CM}} = \delta L/c \quad \text{and} \quad T_{\text{SC1}} = (2\Omega L/c)^2 \quad (3)$$

For a lossless sloshing cavity we can generate an optimised result with an equal sensitivity at high frequencies to the Advanced LIGO design using the following

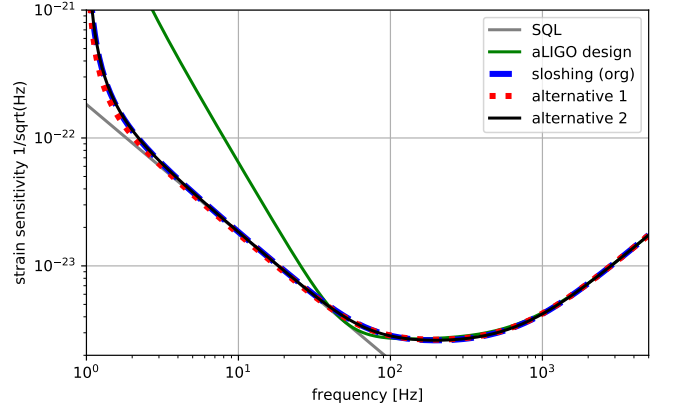


Figure 2. Quantum-limited sensitivity of the Advanced LIGO design with different sloshing cavity designs, the optical parameters are listed in Table I. The design sensitivity of Advanced LIGO (aLIGO) and the Standard Quantum Limit (SQL) are shown for reference.

parameters: $\delta = 2\pi \times 750$ Hz and $\Omega = 2\pi \times 200$ Hz. The quantum-noise limited sensitivity is shown in Figure 2, and the optical parameters are listed in Table I. The sloshing cavity in this example has the same length (3995 m) as the interferometer arm cavities, and has a finesse of $F = 5600$. The quantum-noise-limited sensitivity of the setup shows the typical shape of a speedometer configuration with the quantum noise touching the Standard Quantum Limit (SQL) for a wide range of frequencies, significantly improved over the RSE Michelson.

II. ALTERNATIVE CONFIGURATIONS

We can quickly compare a wide range of optical layouts by using numerical interferometer modelling software such as FINESSE [7, 8]. We used simple analytical derivations for the interferometer bandwidth to find setups which should have an equivalent performance and then confirmed this with a numerical model that does not rely on our assumptions or approximations.

We can achieve the same quantum-noise-limited sensitivity with simplified setups shown in Figures 3 and 4. The layout shown in Figure 3 has two significant changes to the one shown before: a) the Signal Recycling Mirror has been removed and b) the coupling mirror is located inside the sloshing cavity. The immediate advantage of this new setup is that it includes two fewer mirrors and presents a much less complex control problem. We can compute the sloshing frequency and extraction rate in this setup using the reflectivity and transmissivity of the sloshing cavity derived in Appendix B, and Ω is now defined as:

$$\Omega = \frac{c\sqrt{R_{\text{CM}}T_{\text{ITM}}}}{2L} \quad (4)$$

The bandwidth of the system, i.e. the extraction rate δ

will be defined by the combined transmissions through the sloshing cavity T_{SC} and the transmission of the input test masses T_{ITM} .

The reflectivity of the sloshing cavity is (Appendix B):

$$r_{SC} = \frac{1 - T_{CM}}{1 + T_{CM}} \quad (5)$$

And the reflectivity of the coupled cavity formed by the ITM and the sloshing cavity is given as:

$$R_{CC} = \frac{(r_{ITM} - r_{SC})^2}{(1 - r_{ITM}r_{SC})^2}, \quad (6)$$

The half bandwidth of such a cavity is:

$$\gamma = \frac{c}{2L} \frac{1 - R_{CC}}{\sqrt{R_{CC}}} \quad (7)$$

For a given $\gamma = 750 \times 2\pi$ this leads to a quadratic equation for the reflectivity of the coupled cavity with only one real solution: $R_{CC} = 0.778$.

With this result, $\Omega = 200 \times 2\pi$, and from equations 4, 5 and 6 we obtain a cubic equation with only one real solution, from which we obtain the values:

$$T_{CM} = 0.995 \quad \text{and} \quad T_{ITM} = 0.22 \quad (8)$$

And indeed, a numerical search for the optimal parameters, taking into consideration the transmission of the ETMs and surface losses of 37 ppm per surface in the main interferometer, provides very similar values:

$$T_{CM} = 0.996 \quad \text{and} \quad T_{ITM} = 0.228 \quad (9)$$

The resulting quantum-noise-limited sensitivity is shown in Figure 2.

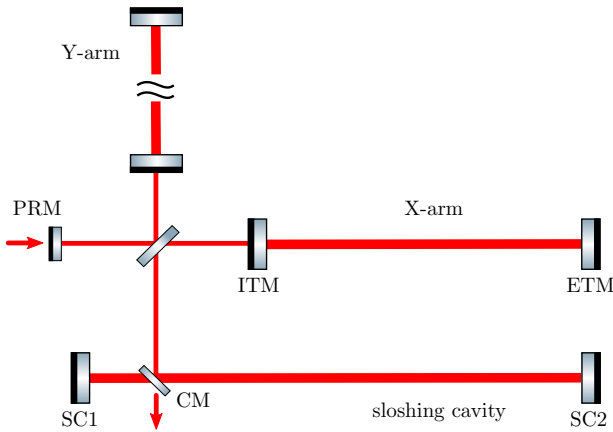


Figure 3. Alternative optical layout for sloshing cavity based on the Advanced LIGO design (sloshing MI).

The new layout has the advantage of using two fewer mirrors but requires a large circulating light power inside the power recycling cavity and thus within the substrate

of the main beam splitter. Instead we can achieve the same sensitivity if we use the same main interferometer parameters as the current Advanced LIGO layout, i.e. a signal recycling mirror with moderate transmission and an arm cavity with a finesse of 450. We can use the fact that the bandwidth of the original signal recycling cavity is already correct and that we have computed the corresponding reflectivity of the coupling mirror already for the first alternative layout.

This optical layout is shown in Figure 4, the resulting parameters for the mirror reflectivities are listed in Table I as ‘sloshing alternative 2’, and the corresponding sensitivity is also shown in Figure 2. This second alternative provides a more practical option: As shown in Table I this configuration leaves the power in the beam splitter unaltered whereas the first alternative requires an almost 20 times higher power in the central beam splitter. Experience at the GEO detector has shown that the thermal distortion in the beam splitter are complex due to the asymmetric beam path [9]. While advanced thermal compensation systems are being investigated, it seems unlikely that alternative 1 would provide sufficiently good contrast defect at the beamsplitter. In the following we will therefore concentrate our investigation on alternative 2.

It should be noted that a general optimisation for detectors with other requirements in terms of power, bandwidth, cavity finesse, etc. can easily be undertaken using numerical models. For example, the optical losses and their effect on the quantum-noise reduction is a key aspect of a more detailed design, see [10].

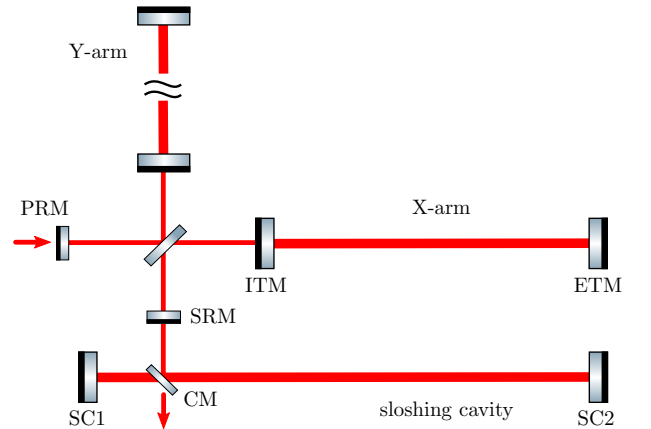


Figure 4. Second alternative optical layout for a sloshing cavity based on the Advanced LIGO design, including a signal recycling mirror and a coupling mirror inside the sloshing cavity.

III. PROPAGATION OF MIRROR POSITION NOISE INTO THE GRAVIATIONAL WAVE CHANNEL

In this section we investigate the noise coupling of the position of the new optical elements, such as the sloshing cavity mirrors, into the gravitational wave channel, i.e. the optical signal detected in the dark port.

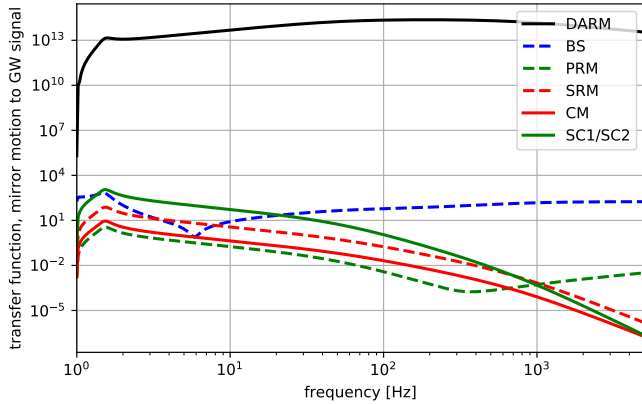


Figure 5. Coupling of mirror displacement into the gravitational wave output channel. The plot shows the coupling of mirror motion of the components of the sloshing cavity (CM, SC1, SC2) and compares it to the coupling of the beamsplitter and recycling mirrors (BS, PRM, SRM). It can be seen that the noise coupling is of similar order of magnitude or smaller (at higher frequencies).

Figure 5 shows the simulated transfer functions for mirror motions, comparing the motion of the sloshing cavity (CM, SC1, SC2) to the coupling of the beamsplitter and recycling mirrors (BS, PRM, SRM). For reference the coupling of a differential end mirror motion (mimicking a gravitational wave signal) is shown as well.

It should be noted that the model does not include any defects, such as unwanted asymmetries in the interferometer arms. Instead we have used a simple method to model the effects of such asymmetries on the noise couplings by applying a small offset to the differential arm length of the interferometer. A so-called DC-offset is used currently by LIGO in order to generate a local oscillator field in the output port [1]. The DC offset is a deliberate deviation from the symmetric system set carefully such that it couples light into the output port with just enough power to dominate over any other light leaking out of the interferometer due to unwanted asymmetries. Therefore the DC offset in the LIGO detectors provides a good indirect measure of the expected unwanted asymmetries we can expect. In the next upgrade the LIGO detectors will be equipped with a homodyne readout systems for which the DC offset is not required. We also assume a homodyne readout for the interferometer layouts presented here. An investigation using an interferometer model without defects but by including the current amount of DC offset allows to mimic the effect of interfer-

ometer defects in a simple and effective way. Using this numerical model we evaluate the relative strength of the coupling between different optics and provides an upper limit for the absolute noise coupling. This result shows that the coupling for the sloshing cavity is at most of similar order of magnitude as the coupling of the optics in the short Michelson interferometer (BS, SRM, PRM). Therefore standard mirror suspension systems will be sufficient for the sloshing cavity optics. Additionally, a sensing and control scheme for the sloshing cavity mirror positions would have to achieve the same level of precision as the control system for the Michelson optics.

We suggest that the alternative configuration proposed in this article should be further investigated for its behaviour in the presence of defects as was done for the Sagnac configuration in [11]. In addition, requirement on the mode matching should be evaluated. Both are beyond the scope of this article.

ACKNOWLEDGMENTS

The presented work was started during the very productive Speed Meter Workshop in 2016, sponsored by the International Max-Planck Partnership Scotland and hosted and organised by Stefan Hild. The authors would like to thank Stefan Danilishin, Yanbei Chen, Paul Fulda and Conor Mow-Lowry for useful comments and discussions. A. Freise has been supported by the Science and Technology Facilities Council (STFC) and by a Royal Society Wolfson Fellowship which is jointly funded by the Royal Society and the Wolfson Foundation. Daniel Brown was supported by the Australian Research Council grant CE170100004.

Appendix A: Detector bandwidth

In the following we recall characteristic parameters as defined in [6], based on the standard notation introduced in [12]. For current detectors the target shape of the quantum-noise-limited sensitivity curve is a wide 'bucket' around an optimal frequency around 100 Hz. The width of the region with low quantum noise is defined by the detector bandwidth, given by the half-bandwidth of the optical cavity storing the optical signal. In case of a Michelson with Fabry-Perot arm cavities this is given by the half-bandwidth of the arm cavities. The half bandwidth, or pole frequency, of such a cavity can be computed as:

$$\gamma = \frac{c}{2L} \arcsin\left(\frac{1 - r_{\text{ITM}}}{\sqrt{r_{\text{ITM}}}}\right) \quad (\text{A1})$$

with T_{ITM} the transmissivity of the input test mass (assuming $T_{\text{ETM}} \ll T_{\text{ITM}}$), c the speed of light and L the length of the arm cavities. In the cases discussed here,

the argument of the arcsin function is usually small so that we can approximate this as:

$$\gamma \approx \frac{c}{2L} \frac{1 - r_{\text{ITM}}}{\sqrt{r_{\text{ITM}}}} \quad (\text{A2})$$

In Advanced LIGO the half bandwidth is given by the half bandwidth of the coupled cavity created by the signal recycling mirror (SRM) and the arm cavity mirrors (ITM, ETM). We can understand the combination of SRM and ITM as one compound mirror M_{SRC} . The power reflectivity and transmissivity of the cavity can be computed as:

$$R_{\text{SRC}} = \frac{R_{\text{ITM}} + R_{\text{SRM}} - 2r_{\text{ITM}}r_{\text{SRM}} \cos(\phi)}{1 + R_{\text{ITM}}R_{\text{SRM}} - 2r_{\text{ITM}}r_{\text{SRM}} \cos(\phi)}, \quad (\text{A3})$$

and

$$T_{\text{SRC}} = \frac{T_{\text{ITM}}T_{\text{SRM}}}{1 + R_{\text{ITM}}R_{\text{SRM}} - 2r_{\text{ITM}}r_{\text{SRM}} \cos(\phi)} \quad (\text{A4})$$

with ϕ the tuning of the cavity. The nominal Advanced LIGO design assumes the SRC to be tuned for resonant signal extraction with $\phi = 0$ and we can simplify:

$$R_{\text{SRC}} = \frac{(r_{\text{ITM}} - r_{\text{SRM}})^2}{(1 - r_{\text{ITM}}r_{\text{SRM}})^2}, \quad T_{\text{SRC}} = \frac{T_{\text{ITM}}T_{\text{SRM}}}{(1 - r_{\text{ITM}}r_{\text{SRM}})^2} \quad (\text{A5})$$

The half bandwidth of the detector, given by the half bandwidth of the cavity formed by the arm and the signal recycling mirror, is then:

$$\gamma \approx \frac{c}{2L} \frac{1 - r_{\text{SRC}}}{\sqrt{r_{\text{SRC}}}} \quad (\text{A6})$$

Purdue and Chen define two quantities to describe the sloshing speedmeter: the sloshing frequency Ω and the signal extraction rate δ as angular frequencies. The sloshing frequency Ω indicates at which frequency the quantum-noise-limited sensitivity will be best and the extraction rate δ is equivalent to the bandwidth γ in the Advanced LIGO layout.

Appendix B: Reflectivity of the sloshing cavity with the coupling mirror inside

To compute the bandwidth of the interferometer in a sloshing configuration we need to know the reflectivity of the sloshing cavity for a light field leaking out of the

interferometer. If the coupling mirror is located inside the sloshing cavity we need to use a slightly different equation than usual for the reflectivity of the cavity.

A sketch of the relevant optical setup is shown in Figure 6. The reflectivity of the sloshing cavity is then defined as $r_{\text{SC}} = E_r/E_0$ and the transmissivity as $t_{\text{SC}} = E_t/E_0$ respectively.

Assuming almost perfectly reflecting mirrors SC1 and SC2, the amplitude reflectivity and transmissivity can

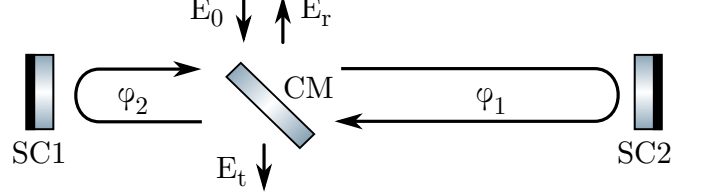


Figure 6. Sketch to show the electric field coupling at the coupling mirror inside the sloshing cavity. E_0 is the incoming field from the main interferometer. φ_1 refers to the phase the light accumulates in the right half of the cavity, φ_2 is for the left half.

be computed from the parameters of the coupling mirrors R_{CM} , T_{CM} and the cavity tunings, given as φ_1 and φ_2 . We use the convention of applying a 90 degrees phase shift on transmission of an optical element and none at reflection as described in [13]. We get:

$$r_{\text{SC}} = \frac{R_{\text{CM}}e^{-i\varphi_1} + R_{\text{CM}}T_{\text{CM}}e^{i\varphi_2}}{1 + T_{\text{CM}}^2} \quad (\text{B1})$$

and

$$t_{\text{SC}} = iT_{\text{CM}} \frac{1 + e^{-i(\varphi_1 + \varphi_2)}}{1 + T_{\text{CM}}e^{i(\varphi_1 + \varphi_2)}} \quad (\text{B2})$$

If the sloshing cavity is on resonance for the carrier light frequency the sum of the phases is known so that

$$\exp(-i(\varphi_1 + \varphi_2)) = -1 \quad (\text{B3})$$

The power coefficient are then independent of the differential tuning:

$$R_{\text{SC}} = \frac{(1 - T_{\text{CM}})^2}{(1 + T_{\text{CM}})^2} \quad (\text{B4})$$

$$T_{\text{SC}} = \frac{4T_{\text{CM}}}{(1 + T_{\text{CM}})^2} \quad (\text{B5})$$

-
- [1] J Aasi et al. (LIGO collaboration). Advanced LIGO. *Classical and Quantum Gravity*, 32(7):074001, 2015. **1, 4**
 - [2] F Acernese et al. (Virgo collaboration). Advanced Virgo: a second-generation interferometric gravitational wave

detector. *Classical and Quantum Gravity*, 32(2):024001, 2015.

- [3] H Grote (for the LIGO Scientific Collaboration). The GEO 600 status. *Classical and Quantum Gravity*,

- 27(8):084003, apr 2010.
- [4] Yoichi Aso, Yuta Michimura, Kentaro Somiya, Masaki Ando, Osamu Miyakawa, Takanori Sekiguchi, Daisuke Tatsumi, and Hiroaki Yamamoto. Interferometer design of the KAGRA gravitational wave detector. *Phys. Rev. D*, 88:043007, Aug 2013. [1](#)
 - [5] M Punturo et al. (ET Science Team). The Einstein Telescope: a third-generation gravitational wave observatory. *Classical and Quantum Gravity*, 27(19):194002, 2010. [1](#)
 - [6] P Purdue and Y Chen. Practical speed meter designs for quantum nondemolition gravitational-wave interferometers. *Physical Review D*, 66(12):122004–+, December 2002. [1](#), [4](#)
 - [7] A Freise, G Heinzl, H Lück, R Schilling, B Willke, and K Danzmann. Frequency-domain interferometer simulation with higher-order spatial modes. *Classical and Quantum Gravity*, 21(5):S1067–S1074, 2004. [2](#)
 - [8] D D Brown and A Freise. Finesse, Frequency domain interferometer simulation software. <http://www.gwoptics.org/finesse>, May 2014. Accessed: 2019-09-09. [2](#)
 - [9] H Wittel, C Affeldt, A Bisht, S Doravari, H Grote, J Lough, H Lück, E Schreiber, K A Strain, and K Danzmann. Matrix heater in the gravitational wave observatory GEO 600. *Opt. Express*, 26(18):22687–22697, Sep 2018. [3](#)
 - [10] S H Huttner, S L Danilishin, S Hild, and K A Strain. Comparison of different sloshing speedmeters. *submitted to CQG*, 2019. [3](#)
 - [11] S L Danilishin, C Gräf, S S Leavey, J Hennig, E A Houston, D Pascucci, S Steinlechner, J Wright, and S Hild. Quantum noise of non-ideal Sagnac speed meter interferometer with asymmetries. *New Journal of Physics*, 17(4):043031, 2015. [4](#)
 - [12] H. J. Kimble, Y. Levin, A. B. Matsko, K. S. Thorne, and S. P. Vyatchanin. Conversion of conventional gravitational-wave interferometers into quantum nondemolition interferometers by modifying their input and/or output optics. *Physical Review D*, 65(2):022002–+, January 2002. [4](#)
 - [13] C Bond, D Brown, A Freise, and K A Strain. Interferometer techniques for gravitational-wave detection. *Living Reviews in Relativity*, 19(1):3, 2017. [5](#)